


Cite this: *RSC Adv.*, 2021, 11, 2546

# Improvement of protein emulsion stability through glycosylated black bean protein covalent interaction with (–)-epigallocatechin-3-gallate†

Jubing Wang,<sup>a</sup> Huanyu Zheng,<sup>bcd</sup> Shenyi Zhang,<sup>a</sup> Jishu Li,<sup>a</sup> Xiuqing Zhu,<sup>e</sup> Hua Jin<sup>\*a</sup> and Jing Xu<sup>id</sup><sup>\*a</sup>

This study investigated the effects of covalent conjugates combined by glycosylated black bean protein isolate (BBPI-G) and (–)-epigallocatechin-3-gallate (EGCG) on the emulsion stability. Fourier transform infrared (FTIR) spectroscopy showed that covalent binding of EGCG with BBPI-G made the protein molecule unfolded. Besides, the emulsifying properties of BBPI-G were increased after combined with EGCG. BBPI-G–EGCG emulsion had lower mean particle size and higher content of interfacial protein adsorption (AP), which resulted in thicker and more impact oil–water interface. Therefore, the stability of emulsions was significantly improved. Furthermore, the emulsions prepared by BBPI-G–EGCG compounds exhibited considerable stability in storage, oxidation, thermal treatments, freeze–thaw and freeze-dried powders resolubility. This study demonstrated that the covalent bond of glycosylated protein and polyphenols could advance the emulsifying performance of protein, and BBPI-G–EGCG covalent complex was an effective emulsifier for preparing high stability emulsions.

Received 14th October 2020

Accepted 2nd January 2021

DOI: 10.1039/d0ra08756d

rsc.li/rsc-advances

## 1. Introduction

The content of black bean protein isolate (BBPI) is remarkable in the total weight of black bean, which is higher than for soybean and even milk.<sup>1</sup> BBPI is rich in essential amino acids (AA), and the balance of AA is commendable.<sup>2</sup> Moreover, it has been investigated that the solubility, emulsifying activity and emulsion stability of BBPI are excellent because of high amounts of hydrophobic amino acids.<sup>3</sup> Thus, BBPI has great potential to stable emulsions in food industry. The oil–water emulsion is kind of delivery system to encapsulate unstable hydrophobic biological active substance (curcumin,  $\alpha$ -tocopherol, *etc.*), which is able to improve stability of ingredients by reducing the exposure of hydrophobic biological active substance to external factors, such as oxygen and light.<sup>4</sup> In the

process of emulsion preparation, the emulsifier can form an interface layer to separate the oil–water phase. The densification, thickness, stability and anti-oxidation of the emulsifier layer will have an important influence on the stability of the emulsion and the encapsulated substance. However, protein is willing to aggregate itself and is susceptible to external environment brought by processing conditions in food industry. Hence, it is needed to improve the functional properties of protein *via* appropriate modification methods.<sup>4</sup>

The interaction of protein and polyphenols is able to change the structure of protein, improve its functional characteristics, and increase the potential value of protein and polyphenols in the field of food industry. Two combination methods between protein and polyphenol are non-covalent interaction and covalent interaction. Li *et al.*<sup>5</sup> reported that non-covalent complexes of (+)-catechin and rice bran protein had lower contents of  $\alpha$ -helix and  $\beta$ -sheet in secondary structure, and formed more stable emulsions with smaller droplet size and greater emulsifying property at additive amount of 0.15% (w/v). Su *et al.*<sup>6</sup> studied that the non-covalent interaction of  $\beta$ -lactoglobulin nanoparticles to (–)-epigallocatechin-3-gallate (EGCG) could increase antioxidant property of protein. Similarly, Loc *et al.*<sup>7</sup> found that the thermal stability and antioxidative capacity of covalent adducts of polyphenol and flaxseed protein isolate were increased. Furthermore, Zhou *et al.*<sup>8</sup> reported that non-covalent interaction and covalent interaction could both change the secondary structure and properties of soybean protein isolate (SPI), while SPI–EGCG covalent complex held more stable structure, better

<sup>a</sup>College of Art and Science, Northeast Agricultural University, 150030 Harbin, Heilongjiang, PR China. E-mail: 15663431982@163.com; zsy123@163.com; ljsy123@163.com; jinhua@neau.edu.cn; xujing@neau.edu.cn

<sup>b</sup>College of Food Science, Northeast Agricultural University, Harbin 150030, Heilongjiang, China. E-mail: zhenghuanyu1@163.com

<sup>c</sup>Heilongjiang Green Food Science Research Institute, Harbin 150028, Heilongjiang, China

<sup>d</sup>National Research Center of Soybean Engineering and Technology, Harbin 150028, Heilongjiang, China

<sup>e</sup>Key Laboratory of Grain Food and Comprehensive Processing of Grain Resource of Heilongjiang Province, College of Food Engineering, Harbin University of Commerce, Harbin 150076, China. E-mail: xqzhuwang@163.com

† Electronic supplementary information (ESI) available. See DOI: 10.1039/d0ra08756d



thermal stability and oxidation resistance than non-covalent complexes.

After glycosylation, the solubility, thermal stability, emulsifying property, foaming property and antioxidant activity of protein can be significantly improved.<sup>9–14</sup> Zha *et al.*<sup>10</sup> reported that pea protein isolate–gum arabic (PPI–GA) complex formed by glycosylating reaction had higher solubility. Laura *et al.*<sup>11</sup> found that glycosylation of whey protein significantly improved the solubility and thermal stability. In recent years, the research of proteins, carbohydrates and polyphenols have all become hot topics. Perusko *et al.*<sup>15</sup> investigated the binding affinity of glycosylated  $\beta$ -lactoglobulin with EGCG through non-covalent interaction and the antioxidant properties of  $\beta$ -lactoglobulin–EGCG non-covalent complex. Results showed that the binding affinity between glycosylated  $\beta$ -lactoglobulin and EGCG was similar to that between  $\beta$ -lactoglobulin and EGCG. However, antioxidant capacity of glycosylated  $\beta$ -lactoglobulin–EGCG non-covalent complex was higher, revealing that the combination of carbohydrate and polyphenols significantly increased the antioxidant properties of  $\beta$ -lactoglobulin. Meanwhile, the combination of carbohydrate and polyphenols showed synergistic and superimposed effects. Liu *et al.*<sup>16</sup> researched the application of lactoferrin (LF), glucan and chlorogenic acid (CA) ternary complex through covalent interaction as emulsifier in emulsion. The results indicated that preparative ternary complex showed greater emulsification property and antioxidant activity than LF or LF–CA binary complex. The reason was that LF maintained surface activity of emulsion system as emulsifier, and the combination of carbohydrate and polyphenols enhanced spatial repulsive force and antioxidant capacity of emulsion system, respectively.

Many studies have shown that proteins, carbohydrates and polyphenols can coexist by interacting with each other in different ways, and the formation of ternary complexes can further advance protein functional properties.<sup>17</sup> Nevertheless, to the best of our knowledge, the effects of covalent interaction between glycosylated proteins and polyphenols on the stability of emulsion has been rarely reported, and little information is available on the relevance between the changes of protein structure and emulsion stability. Therefore, a better understanding of the interaction between glycosylated proteins–polyphenol emulsifiers and emulsion properties would help to optimize protein application in food products during processing and storage. BBPI was chosen as the research subject in this study. The effects of covalent interaction between glycosylated BBPI (BBPI–G) and EGCG on the structure and properties of protein complexes were studied on the first aspect, comparing with the native BBPI as control. The emulsions were then prepared by BBPI, BBPI–G, BBPI and EGCG covalent complex (BBPI–EGCG), BBPI–G and EGCG covalent complex (BBPI–G–EGCG). The effects of glycosylation modification and polyphenols modification on the basic and stability properties of emulsions were explored. The relationship between protein structure and emulsion stability was discussed.

## 2. Materials and methods

### 2.1. Materials

BBPI were purchased from Hei Long Jiang Agriculture Company Limited (Hei Long Jiang, China). Glucose was bought from Baolingbao Biology Company (Shandong, China). (–)-Epigallocatechin-3-gallate (EGCG) was received from Yuanye Biotechnology Co. Ltd (Shanghai, China). Soya oil of gold arowana was obtained from Yihai Kerry Foodstuffs Marketing Company (Jiangsu, China). All other chemical medicines were of analytical grade.

### 2.2. Preparation of Maillard reaction compounds

A ratio of 2 : 1 (BBPI : G, w/w) of BBPI and glucose was dissolved in phosphate buffer (0.1 M, pH 7.0). Wet-Maillard reaction was executed (80 °C, 4 h) and then freeze-dried. The graft degree (DG) of 18.83% was determined by our previous study under this condition.<sup>18</sup>

### 2.3. Preparation of phenolic compounds

Freeze-dried powder of BBPI and BBPI–G was dissolved in phosphate buffer (0.01 M, pH 9.0). The protein solution (4 mg mL<sup>−1</sup>) was mixed with EGCG and the ultimate concentration of EGCG were (5, 25, 50, 150, 250  $\mu$ mol g<sup>−1</sup> protein), respectively. The mixture was incubated (25 °C, 12 h) for obtaining BBPI–EGCG and BBPI–G–EGCG covalent compounds.<sup>19</sup> Then, the solution pH was regulated to 7.0. The reactive complex solutions were placed in 3500 kDa dialysis bag and dialysed in phosphate buffer (0.01 M, pH 7.0) for 48 h for removing the free polyphenols. Finally, above solutions were freeze-dried.

### 2.4. Measurement of polyphenol binding rate

With reference to the method of Slinkard *et al.*,<sup>20</sup> the Folin–Ciocalteu method was used to determine the polyphenol binding rate of protein–polyphenol complex samples. 2 mL Folin–Ciocalteu reagent (0.2 mol L<sup>−1</sup>) was added to 0.5 mL protein–polyphenol complex solution at a certain concentration, and the reaction was incubated at 25 °C for 5 min (away from light). Then, 2 mL of Na<sub>2</sub>CO<sub>3</sub> solution (7.5%, w/v) was added to the mixture. The solution was thoroughly mixed with a vortex mixer, and reacted at 25 °C for 2 h (dark). The absorbance of the solution was determined at 760 nm. The standard solution of EGCG with different concentrations was prepared to draw the standard curve, and the polyphenol contents in the complex were calculated according to the standard curve. The polyphenol binding rate was calculated through following formula:

Polyphenol binding rate (%) =

$$\frac{\text{polyphenol content in the compound}}{\text{total polyphenol content}} \times 100\%$$

### 2.5. Fluorescence spectroscopy

The measurement of fluorescence spectroscopy was slightly modified according to Wang *et al.*<sup>21</sup> Sample solutions were diluted to 0.02 mg mL<sup>−1</sup> with the phosphate buffer (0.01 M, pH

7.0). Then, the emission spectrum (slit width 5) from 300 to 550 nm was scanned with excitation wavelength 290 nm using the fluorescence spectrometer of F-4500 (Hitachi, Japan).

## 2.6. Fourier transform infrared (FTIR) spectroscopy

FTIR of BBPI, BBPI-EGCG, BBPI-G, BBPI-G-EGCG were acquired with Bruker Vertex 70 FTIR spectrometer (Bruker Optics, Ettlingen, Germany). The wavenumber was ranging between 4000–400  $\text{cm}^{-1}$ . Spectroscopy data were the average results of 64 scans with a resolution of 4  $\text{cm}^{-1}$ . Select the range of 1600–1700  $\text{cm}^{-1}$  on FTIR spectroscopy. Then, the data was fit to receive 8 groups of area under homologous wavenumbers by “Gaussian peak fitting” algorithm to obtain the percentage contents of four secondary structure by the software “Peakfit Version 4.12”.<sup>22</sup>

## 2.7. Emulsifying properties

The emulsifying activity index (EAI) and emulsifying stability index (ESI) were detected by the method of Jin *et al.*<sup>23</sup> 3 : 1 (v/v) ratio of sample solution (1 mg  $\text{mL}^{-1}$ ) and soybean oil was taken, and homogenized the mixture (10 000 rpm, 2 min). 40  $\mu\text{L}$  liquid were at once absorbed from the emulsion bottom at 0 min and 10 min, which were then added into 5 mL of SDS solution (0.1%, w/v). Suspensions after shock blending were detected at 500 nm. Computational formula for calculating EAI and ESI were as follows:

$$\text{EAI} (\text{m}^2 \text{ g}^{-1}) = \frac{2T \times A_0 \times N}{\phi \times L \times C \times 10\,000},$$

$$\text{ESI} (\text{min}) = \frac{A_0 \times t}{A_0 - A_{10}},$$

where  $T$  was 2.303.  $A_0$  and  $A_{10}$  were the absorbance of the emulsion at 0 and 10 min, respectively.  $N$  was dilution factor (125).  $\phi$  was the oil volume fraction (0.25).  $L$  was path length of cuvette (1 cm).  $C$  was protein concentration ( $\text{g mL}^{-1}$ ),  $t$  was sampling interval (10 min).

## 2.8. Preparation of emulsions

400 mg sample powder was accurately weighed and dissolved adequately in 20 mL phosphate buffer (0.02 M, pH 7.0). Soybean oil was slowly added to the protein solution with a ratio of 3% (v/v), stirred magnetically at 25 °C for 10 min, and sodium azide (0.004%, w/v) was added for preventing microbial growth. The coarse emulsion was prepared by homogeneous dispersion machine at 10 000 rpm for 4 min. The coarse emulsion was immediately dealt with an ultrasonic processor (titanium probe with a diameter of 0.636 cm) at 500 W ultrasonic power for 20 min to form emulsion. During the whole preparation process, the temperature was kept at about 25 °C by using ice water bath.<sup>24</sup>

## 2.9. Mean particle size, zeta-potential measurements

Phosphate buffer (0.01 M, pH 7.0) was used to dilute (100 times) the emulsions for ensuring uniformity and avoiding the effects

of multiple scattering. Dynamic light scattering instrument (Malvern Nano-S90, Malvern Instruments, Worcestershire, UK) was used to detect the mean particle size and polydispersity index (PDI). Particle microelectrophoresis (Zetasizer Nano Z, Malvern Instruments, Worcestershire, UK) was selected to measure the zeta-potential.<sup>25</sup>

## 2.10. The percentage of interfacial protein adsorption (AP) measurements

According to Chen *et al.*,<sup>26</sup> emulsion AP was determined with tiny variation. The emulsion was centrifuged (10 000 rpm, 60 min). Acquired aqueous phase from the bottom was sucked with disposable syringe and filtered it to pass 0.45  $\mu\text{L}$  filter membrane. The protein concentration was determined by Lowry method.<sup>27</sup> The protein dispersion was centrifuged under the same conditions. The computational formula of AP was as follows:

$$\text{AP} (\%) = \frac{C_s - C_f}{C_0} \times 100\%,$$

where  $C_f$  was the protein concentration of filtered subnatant from emulsion,  $C_s$  was the protein concentration of centrifugal supernatant from protein dispersion,  $C_0$  was the protein concentration of initial protein dispersion.

## 2.11. Storage stability of emulsions

Different emulsion samples were stored at 4 °C for 30 days, and the storage stability of emulsions was analyzed by measuring the change of mean particle size of emulsions at 0, 10, 20 and 30 days.<sup>9</sup>

## 2.12. Oxidation stability of emulsions

Different emulsion samples were stored at 4 °C for 30 days, and peroxide value (POV) and thiobarbituric acid reactive substances (TBARS) values of the emulsion were measured every 10 days. The oxidation stability of the emulsion was analyzed by the changes of POV and TBARS values.

POV was determined according to the AOCS standard procedure with a sodium thiosulphate ( $\text{Na}_2\text{S}_2\text{O}_3$ ) titration.<sup>29</sup> 0.2 mL emulsion samples were fully mixed by vortex for 1 min with 1.5 mL mixed solution of isopropanol and isooctane (1 : 3, v/v). The mixtures were centrifuged (4000 rpm, 30 min). Later, mix 0.2 mL supernatant and 2.8 mL the mixture of methanol and *n*-butyl alcohol (2 : 1, v/v). Then, 15  $\mu\text{L}$  ammonium thiocyanate solution (3.94 M) and 15  $\mu\text{L}$  bivalent iron ion solution were added, which was prepared by 1 mL of barium chloride solution (0.13 M) and 1 mL of ferrous sulfate solution (0.14 M). The mixture was centrifuged for 3 min at 3000 rpm and left for 20 minute reaction at room temperature away from light. The absorbance of the solution was determined at 510 nm. POV values of emulsion samples were calculated by using standard curve of hydrogen peroxide isopropyl benzene.

According to the method described by Mei *et al.*,<sup>30</sup> the formation of TBARS was measured. TBARS value is expressed as malondialdehyde content. 2 mL mixed solution of TCA–TBA–HCl solution (0.92 M TCA, 0.02 M TBA and 1.8% (v/v) HCl) and



BHT-ethanol solution (2%, v/v) (100 : 3, v/v) was added into 2 mL emulsion sample. Mixture was heated in boiling water for 15 min. After cooling to 25 °C, the supernatant was centrifuged (4000 rpm, 10 min). The absorbance of the supernatant was measured at 532 nm. The TBARS values of emulsion samples were calculated by using the standard curve of malondialdehyde.

### 2.13. Thermal stability of emulsions

Emulsion samples were disposed in the boiling water for 10 min or 30 min, and then cooled to 25 °C. The changes of mean particle size were investigated to analyze thermal stability of emulsions.<sup>24</sup>

### 2.14. Freeze-thaw stability of emulsions

Different emulsion samples were frozen in a refrigerator (−20 °C, 20 h), and then thawed for 2 h to analyze the freeze-thaw stability of emulsions by measuring the changes of mean particle size of emulsion.<sup>31</sup>

### 2.15. Resolubility of freeze-dried emulsion powders

The emulsion samples were freeze-dried into powder and then dissolved back to the original volume with phosphate buffer (0.01 M, pH 7.0). The resolubility of the powder was analyzed by measuring the changes of mean particle size of the emulsions.<sup>32</sup>

### 2.16. Statistical analysis

All the tests were measured in triplicate. The results were showed as shape of mean  $\pm$  standard deviation. ANOVA significance analysis ( $p < 0.05$ ) and independent sample *T* test (*T*) ( $p < 0.05$ ) were proceeded with statistical software (SPSS V20.0) to display significant differences.

## 3. Results and discussion

### 3.1. Structure and functional properties

**3.1.1. Polyphenol binding rate.** Polyphenol binding rate reflects to the combining quantity of polyphenol in protein-polyphenol complexes. Fig. 1 showed a polyphenol binding rate tendency of rising and then falling with the increase of EGCG concentration in both BBPI group and BBPI-G group. When the polyphenol concentration increased to 150  $\mu\text{mol g}^{-1}$  protein, the polyphenol binding rate in the BBPI-EGCG and BBPI-G-EGCG covalent complexes reached the maximum value, which was  $93.17 \pm 2.55\%$  and  $96.96 \pm 1.17\%$ , respectively. The result indicated that a valid conjugation of BBPI and BBPI-G with EGCG occurred. At concentration of 250  $\mu\text{mol g}^{-1}$  protein, polyphenol binding rate decreased, because the increasing of binding amount was slower than the increasing of EGCG additive amount. Hence, the binding rate was reduced after calculation. Sui *et al.*<sup>33</sup> showed similar conclusion by studying covalent binding of soybean protein isolate with anthocyanin. The higher maximum value in BBPI-G-EGCG group than BBPI-EGCG manifested that BBPI had better reactivity with EGCG after glycosylation. It was reported that the number and

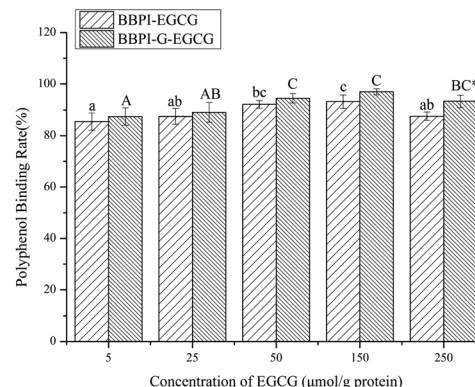


Fig. 1 Polyphenol binding rate of BBPI and BBPI-G samples with different concentration of EGCG (5, 25, 50, 150 and 250  $\mu\text{mol g}^{-1}$  protein). a–c represents significant difference in BBPI with different EGCG concentrations ( $p < 0.05$ ). A–C represents significant difference in BBPI-G with different EGCG concentrations ( $p < 0.05$ ). \* means significant difference between BBPI and BBPI-G ( $p < 0.05$ ).

position of hydroxyl groups in protein could possibly influence reaction activity of oxydic polyphenol and protein.<sup>16</sup> Therefore, more hydroxyl groups and exposure of binding sites after glycosylation led to an increasing reactivity of polyphenol and glycosylated protein.

**3.1.2. Fluorescence spectroscopy.** Tryptophan (Trp) and tyrosine (Tyr) in protein was used as a fluorescent probe in fluorescence spectroscopy measurement to research tertiary structure of protein conformation. Fig. 2 displayed curve changes of BBPI and BBPI-G when adding various amount of EGCG. All  $\lambda_{\text{max}}$  were superior to 330 nm. Research had shown that Trp was inside of protein molecules if  $\lambda_{\text{max}} < 330$  nm and in external polarity environment if  $\lambda_{\text{max}} > 330$  nm.<sup>14</sup> Meanwhile, maximum values of fluorescence spectroscopy declined significantly and red-shifts phenomenon occurred by rising the amount of EGCG in Fig. 2a and b. Decline of intensity value confirmed that fluorescence quenching appeared as EGCG was added to BBPI and BBPI-G. This was because polyphenols were readily oxidized into electrophilic quinones, which interacted more strongly with tryptophan and tyrosine residues in proteins, binding with more hydrophobic amino acids and resulting decline of Trp amount.<sup>16,34</sup> Red-shifts meant that more hydrophobic residues were exposed to outside surroundings or transfer to hydrophilic environment effected by EGCG.<sup>13</sup>

Compared Fig. 2a with Fig. 2b, it was not difficult to discover that declining degree of intensity and red-shift of BBPI-G-EGCG surpassed BBPI-EGCG. On one side, the lower fluorescence intensity was attributed to the fact that glycosylation was accompanied with the shielding effect and more hydrophobic residues were buried by the polysaccharide molecules.<sup>18</sup> Meanwhile, the covalent binding of polyphenols led to the quenching of fluorescence intensity of glycosylated BBPI, which might be related to Forster-type fluorescence resonance energy transfer.<sup>17</sup> On the other side, the  $\lambda_{\text{max}}$  values of BBPI-G-EGCG in Fig. 2b were larger than those in Fig. 2a, showing that BBPI-G-EGCG red-shifted more obviously compared with BBPI-EGCG,



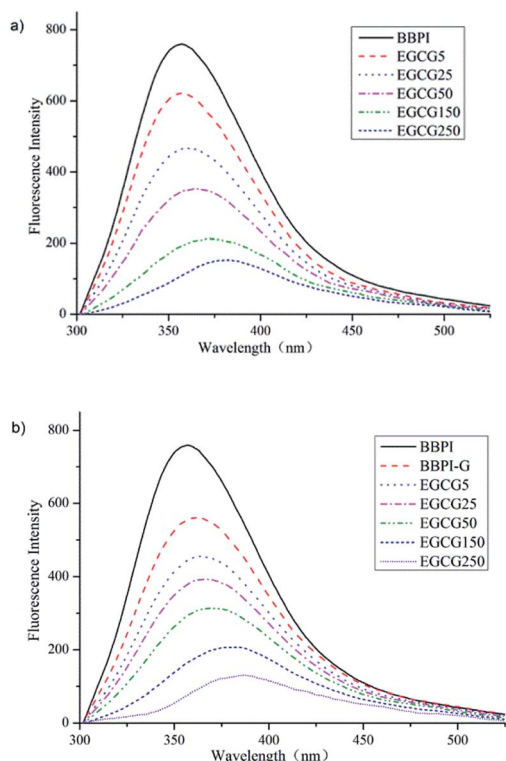


Fig. 2 Fluorescence spectroscopy curve of BBPI-EGCG (a) and BBPI-G-EGCG (b) with EGCG amount of 5, 25, 50, 150 and 250  $\mu\text{mol g}^{-1}$  protein.

which meant that BBPI-G-EGCG might have more incompact structure than BBPI-EGCG.<sup>28</sup>

**3.1.3. Fourier transform infrared (FTIR) spectroscopy.** FTIR is a basic measurement in detecting characteristic functional group of chemical construction. Changes of amide I band ( $1600\text{--}1700\text{ cm}^{-1}$ ) shows the variation of the secondary structure of protein, which contains  $\alpha$ -helix ( $1650\text{--}1660\text{ cm}^{-1}$ ),  $\beta$ -sheet ( $1610\text{--}1640\text{ cm}^{-1}$ ),  $\beta$ -turn ( $1660\text{--}1700\text{ cm}^{-1}$ ) and random coil ( $1640\text{--}1650\text{ cm}^{-1}$ ) after analyzed through second derivative fitting. As shown in Table 1, the content of  $\beta$ -turn in BBPI-G was higher than that in BBPI, while the other secondary structure of BBPI-G decreased compared with BBPI. The result explained that secondary structure of BBPI went to a disordered direction. Destruction of secondary structure was due to the changes of van der Waals forces and hydrogen bonding among protein molecules influenced by glycosylation.<sup>28</sup> Covalent binding of EGCG made a further structure disorder of both BBPI and BBPI-G as observed in Table 1. The  $\alpha$ -helix and  $\beta$ -sheet content in BBPI and BBPI-G both reduced with increasing content of EGCG, while the  $\beta$ -turn and random coil content enlarged, owing to the reaction of oxydic phenol product and glycinin protein *via* amino, thiol groups and tryptophan.<sup>35</sup> Similar conclusion was reported by Wei *et al.*,<sup>36</sup> which investigated the structure and function properties of EGCG-milk conjugations. The author explained that the change of  $\alpha$ -helix,  $\beta$ -sheet,  $\beta$ -turn and random coil indicated that EGCG binding made protein secondary structure destruct.

**3.1.4. Emulsifying properties.** Emulsifying property is one of the important functional properties of protein, which affects the application of protein in food industry. As was displayed in Fig. 3, EAI and ESI of BBPI-EGCG and BBPI-G-EGCG covalent complexes were higher than those of BBPI and BBPI-G. Moreover, EAI and ESI of BBPI-G-EGCG group were higher than BBPI-EGCG group. This was due to the combination of EGCG hydroxyl groups and the amino acid residues of proteins (BBPI and BBPI-G), which led to the conformational stretching of proteins. Hence, the water binding ability of modified protein was improved, making it a better hydrophilic and hydrophobic balance and enhancing the adsorption ability of protein onto the oil-water interface. Therefore, the emulsifying ability of BBPI and BBPI-G was improved.<sup>36</sup> Moreover, EAI and ESI of BBPI-G-EGCG group were higher than BBPI-EGCG group. One reason of the difference was that glycosylation improve the surface property and emulsifying property of protein, which also impacted BBPI-G-EGCG.<sup>37</sup> The other reason might be the higher polyphenol binding rate of BBPI-G-EGCG, which gave BBPI-G-EGCG better emulsifying capacity.

## 3.2. Emulsion properties

**3.2.1. Mean particle size, zeta-potential.** According to Fig. 3, it could be found that the protein-polyphenol compounds show the best emulsifying capacity at the polyphenol concentration of  $150\text{ }\mu\text{mol g}^{-1}$  EGCG/protein. Therefore, BBPI-EGCG 150 and BBPI-G-EGCG 150 were chosen as the emulsifiers to stabilize the emulsion system and compared with BBPI and BBPI-G. Mean particle size and zeta-potential of emulsions are common indexes to measure stability of emulsions. In general, small mean particle size accompanied with better emulsion stability and properties. Zeta-potential reflected charge quantity on the surface of protein. The higher absolute zeta-potential value of protein, the higher electrostatic repulsion maintained. Thus, higher energy barrier among emulsion droplets insisted, providing more stable emulsion.<sup>45</sup> In Table 2, the absolute zeta-potential value of BBPI-EGCG was  $30.90 \pm 0.26\text{ mV}$  growing from  $24.47 \pm 0.23\text{ mV}$  of BBPI, and value of BBPI-G-EGCG ( $29.47 \pm 0.61\text{ mV}$ ) was also higher than BBPI-G ( $23.20 \pm 0.17\text{ mV}$ ). The results indicated that high electrostatic repulsion observed from zeta-potential measurement led to stable emulsion with small mean particle size. The increase of electrostatic repulsion was attributed to EGCG covalent bound on proteins, which promoted intermolecular repulsion among oil droplets.<sup>38</sup> Moreover, incompact protein complexes provided hydrophobic group to induced better hydrophilic and hydrophobic balance, leading to higher adsorption of protein on interface and forming more stable layer on the surface of oil droplets and emulsions became more stable.<sup>39</sup> However, zeta-potential absolute value of BBPI-G and BBPI-G-EGCG were smaller than BBPI and BBPI-EGCG, respectively, while mean particle size of BBPI-G and BBPI-G-EGCG were smaller. Opposite result between zeta-potential and mean particle size was due to the shielding effect of glycosylation, which was another factor to influence emulsion stability. The shielding effect resulted in the lower zeta-potential, but the carbohydrates



Table 1 Secondary structures of BBPI and BBPI-G with different EGCG concentrations<sup>a</sup>

	$\alpha$ -Helix (%)	$\beta$ -Sheet (%)	$\beta$ -Turn (%)	Random coil (%)
BBPI	16.84 $\pm$ 0.12 <sup>c*</sup>	38.29 $\pm$ 0.08 <sup>d*</sup>	28.74 $\pm$ 0.10 <sup>a</sup>	16.13 $\pm$ 0.04 <sup>a*</sup>
BBPI-EGCG5	16.37 $\pm$ 0.11 <sup>d*</sup>	38.10 $\pm$ 0.08 <sup>c*</sup>	28.96 $\pm$ 0.09 <sup>b</sup>	16.57 $\pm$ 0.01 <sup>b*</sup>
BBPI-EGCG25	16.03 $\pm$ 0.15 <sup>c*</sup>	38.07 $\pm$ 0.07 <sup>c*</sup>	29.09 $\pm$ 0.13 <sup>b</sup>	16.81 $\pm$ 0.07 <sup>c*</sup>
BBPI-EGCG50	15.32 $\pm$ 0.16 <sup>b*</sup>	37.30 $\pm$ 0.14 <sup>b*</sup>	30.30 $\pm$ 0.06 <sup>c</sup>	17.08 $\pm$ 0.18 <sup>d*</sup>
BBPI-EGCG150	14.65 $\pm$ 0.07 <sup>a</sup>	36.94 $\pm$ 0.10 <sup>a*</sup>	30.52 $\pm$ 0.09 <sup>d</sup>	17.89 $\pm$ 0.24 <sup>e*</sup>
BBPI-EGCG250	14.53 $\pm$ 0.08 <sup>a</sup>	36.79 $\pm$ 0.08 <sup>a*</sup>	30.64 $\pm$ 0.10 <sup>d</sup>	18.04 $\pm$ 0.06 <sup>e*</sup>
BBPI-G	15.94 $\pm$ 0.08 <sup>d</sup>	35.99 $\pm$ 0.06 <sup>d</sup>	33.77 $\pm$ 0.08 <sup>a*</sup>	14.30 $\pm$ 0.10 <sup>a</sup>
BBPI-G-EGCG5	15.79 $\pm$ 0.07 <sup>d</sup>	35.84 $\pm$ 0.11 <sup>c</sup>	33.84 $\pm$ 0.10 <sup>a*</sup>	14.53 $\pm$ 0.06 <sup>a</sup>
BBPI-G-EGCG25	15.16 $\pm$ 0.11 <sup>c</sup>	35.66 $\pm$ 0.06 <sup>b</sup>	33.93 $\pm$ 0.07 <sup>a*</sup>	15.25 $\pm$ 0.10 <sup>b</sup>
BBPI-G-EGCG50	14.93 $\pm$ 0.14 <sup>b</sup>	35.60 $\pm$ 0.07 <sup>b</sup>	34.19 $\pm$ 0.07 <sup>b*</sup>	15.28 $\pm$ 0.10 <sup>bc</sup>
BBPI-G-EGCG150	14.63 $\pm$ 0.10 <sup>a</sup>	35.41 $\pm$ 0.09 <sup>a</sup>	34.44 $\pm$ 0.11 <sup>c*</sup>	15.52 $\pm$ 0.19 <sup>cd</sup>
BBPI-G-EGCG250	14.48 $\pm$ 0.13 <sup>a</sup>	35.29 $\pm$ 0.05 <sup>a</sup>	34.55 $\pm$ 0.14 <sup>c*</sup>	15.68 $\pm$ 0.27 <sup>d</sup>

<sup>a</sup> a–e represents significant difference in the same protein with different EGCG concentrations ( $p < 0.05$ ). \* means significant difference between BBPI and BBPI-G ( $p < 0.05$ ).

enhanced the steric hindrance among emulsion droplets to possess better stability.<sup>33</sup> Hence, BBPI-G and BBPI-G-EGCG made more stable emulsion with smaller mean particle size than BBPI and BBPI-EGCG, respectively.

PDI value can reflect the uniformity of emulsion droplet size, and in general, small PDI value usually means narrow droplet size distribution.<sup>40</sup> As shown in Table 2, PDI values of BBPI, BBPI-EGCG, BBPI-G, BBPI-G-EGCG emulsions were  $0.220 \pm 0.007^b$ ,  $0.186 \pm 0.011^a$ ,  $0.187 \pm 0.009^a$ ,  $0.172 \pm 0.008^a$ , respectively. PDI values of four emulsions were all below 0.220, which indicated that uniform emulsions with narrow droplet size distribution were received. Besides, PDI values of BBPI-EGCG, BBPI-G, BBPI-G-EGCG emulsions were significantly smaller than BBPI emulsion ( $p < 0.05$ ), explaining that glycosylation and polyphenol binding could not only reduce the mean particle size of emulsion, but also improve the droplet distribution to achieve the more uniform emulsion with better stability.<sup>41</sup>

### 3.2.2. Percentage of the interfacial protein adsorption (AP).

The contents of interface protein on membrane and dissociative

protein in water phase could also influence thickness and stability of emulsion interfacial membranes. AP of BBPI, BBPI-EGCG, BBPI-G, BBPI-G-EGCG emulsions were  $9.52 \pm 0.29\%$ ,  $18.11 \pm 0.57\%$ ,  $10.53 \pm 0.38\%$ ,  $20.61 \pm 0.76\%$ , respectively, as shown in Table 2. EGCG could increase AP due to the fact that it modified protein structure to unfolded and disordered direction, which resulted in the fast adsorption and tight interaction of molecules on oil–water interface to form the thicker emulsifiers layer.<sup>34,42</sup> Atares *et al.*<sup>43</sup> reported that rutin molecules layer could assist to form thicker films of whey protein emulsion.

For the increase of AP in BBPI-G group, Maillard cross-linking promoted molecular weight, making the thicker film. In addition, hydrophilic group of sugar offered a better hydrophilic and hydrophobic equilibrium, leading to a lifting adsorption amount on oil–water membrane.<sup>10,44</sup> AP of BBPI-EGCG and BBPI-G-EGCG emulsions was superior to BBPI and BBPI-G emulsions, indicating that glycosylation modification had synergistic effect with EGCG covalent binding on the amount of protein adsorption on emulsion interface.

### 3.3. Emulsion stability measurements

**3.3.1. Storage stability of emulsions.** The storage stability of emulsion is an important factor to determine its application in industrial production. As displayed in Fig. 4, the mean particle size of the emulsion prepared with BBPI increased significantly with 10 days of storage ( $p < 0.05$ ). With 20 days of storage, the mean particle size of BBPI-G emulsion enhanced significantly ( $p < 0.05$ ). After 30 days of storage, the mean particle size of BBPI-EGCG covalent compound emulsion increased significantly ( $p < 0.05$ ). However, the mean particle size of BBPI-G-EGCG covalent complex emulsion had no significantly changes during the whole storage period ( $p > 0.05$ ). There were two main reasons induced this result. Firstly, the addition of hydrophilic glucose and polyphenols enhanced the affinity between proteins and water molecules, making it formed a relatively tight interface membrane on the oil drop surface, thus effectively avoiding droplet aggregation and enhancing the storage stability of the emulsion.<sup>9,45</sup> Secondly, the

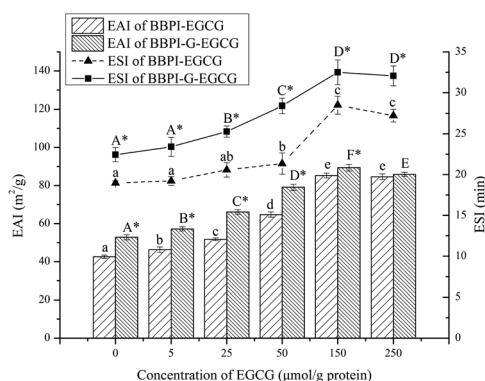


Fig. 3 EAI and ESI of BBPI and BBPI-G compounds with different EGCG concentration (5, 25, 50, 150 and 250  $\mu\text{mol g}^{-1}$  protein). a–e represents significant difference in BBPI with different EGCG concentrations ( $p < 0.05$ ). A–D represents significant difference in BBPI-G with different EGCG concentrations ( $p < 0.05$ ). \* means significant difference between BBPI and BBPI-G ( $p < 0.05$ ).



Table 2 Mean particle size, PDI, zeta-potential, AP of BBPI and BBPI compounds<sup>a</sup>

	Mean particle size (nm)	PDI	Zeta-potential (mV)	AP (%)
BBPI	291.30 ± 0.56 <sup>d</sup>	0.220 ± 0.007 <sup>b</sup>	−24.47 ± 0.23 <sup>b</sup>	9.52 ± 0.29 <sup>a</sup>
BBPI-EGCG	242.17 ± 2.62 <sup>b</sup>	0.186 ± 0.011 <sup>a</sup>	−30.90 ± 0.26 <sup>d</sup>	18.11 ± 0.57 <sup>c</sup>
BBPI-G	282.73 ± 0.35 <sup>c</sup>	0.187 ± 0.009 <sup>a</sup>	−23.20 ± 0.17 <sup>a</sup>	10.53 ± 0.38 <sup>b</sup>
BBPI-G-EGCG	229.67 ± 2.87 <sup>a</sup>	0.172 ± 0.008 <sup>a</sup>	−29.47 ± 0.61 <sup>c</sup>	20.61 ± 0.76 <sup>d</sup>

<sup>a</sup> a–d represents significant difference in the same column ( $p < 0.05$ ).

covalent binding of polyphenols increased the thickness of the droplet interface film and the zeta-potential (absolute value), thereby maintaining the stability of the emulsion by stronger steric resistance and electrostatic repulsion.<sup>46</sup> Wang *et al.*<sup>46</sup> studied the effect of the interaction between corn proteolytic substance (ZH) and tannic acid (TA) on the alginate emulsion system. The results showed that the emulsion prepared by ZH–TA composite had better storage stability.

**3.3.2. Oxidation stability of emulsions.** POV (primary) and TBARS (secondary) are two products in lipid oxidation produce, so that values of POV and TBARS are common detective measure of lipid oxidation extent.<sup>47</sup> Fig. 5a and b showed POV and TBARS increased remarkably with storage time expanded, indicating that lipid oxidation appeared and then rose during storage. Comparing four emulsion groups stabilized by different protein, POV value of the emulsion prepared with BBPI-G-EGCG covalent compound did not show significant change ( $p > 0.05$ ). Regarding as POV, BBPI-G-EGCG emulsion were from  $0.56 \pm 0.01$  meq. kg<sup>−1</sup> oil to  $0.58 \pm 0.01$  meq. kg<sup>−1</sup> oil and then BBPI-EGCG emulsion from  $0.75 \pm 0.02$  meq. kg<sup>−1</sup> oil to  $0.94 \pm 0.03$  meq. kg<sup>−1</sup> oil, BBPI-G emulsion from  $0.91 \pm 0.01$  meq. kg<sup>−1</sup> oil to  $1.45 \pm 0.02$  meq. kg<sup>−1</sup> oil, BBPI emulsion from  $1.19 \pm 0.00$  meq. kg<sup>−1</sup> oil to  $1.81 \pm 0.01$  meq. kg<sup>−1</sup> oil. It showed simultaneously that the smallest value of POV and TBARS belonged to BBPI-G-EGCG emulsion, and then BBPI-EGCG, BBPI-G, BBPI emulsions. The phenomenon illustrated that BBPI-G-EGCG emulsion had the topmost oxidation stability.

Combing with EGCG, protein gained greater oxidation stability, which was attributed to the antioxidative polyphenolic group to scavenging free radicals.<sup>48</sup> Glycosylation introduced hydrophilic glucose to improve the affinity between proteins and water molecules, forming compact film around oil droplets to enhance oxidation stability of emulsions.<sup>49</sup> And the loose and disordered structure of protein caused by glucose and EGCG covalent binding consequently exposed reactive amino acid side-chain groups to neutralizing radicals, leading to an increase in the antioxidant protection.<sup>50</sup> Besides, glucose and EGCG might act as cross-linker to enhance the protein–protein interaction at oil–water interfacial layer.<sup>51</sup> Therefore, glycosylation and EGCG combination could both enhance the emulsion oxidative stability of BBPI and two different modification methods made corporate effect in preventing emulsion oxidation.

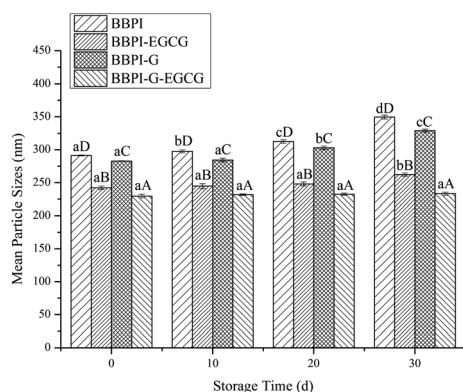


Fig. 4 Mean particle size of BBPI, BBPI-EGCG, BBPI-G, BBPI-G-EGCG emulsions in different storage time (0, 10, 20 and 30 days) at room temperature. a–d represent the significant difference in different storage time with same emulsion (d). A–D means the significant difference in different emulsions with same storage time.

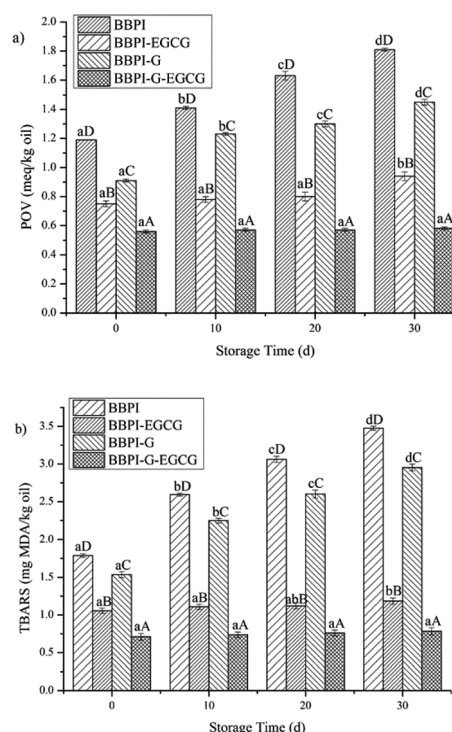


Fig. 5 Oxidation degree of BBPI, BBPI-EGCG, BBPI-G, BBPI-G-EGCG emulsions in different oxidation time (0, 10, 20 and 30 days) at room temperature. (a) peroxide value (POV); (b) thiobarbituric acid reactive substances (TBARS). a–d represent the significant difference in different oxidation time (d) with same emulsion. A–D means the significant difference in different emulsions with same oxidation time.





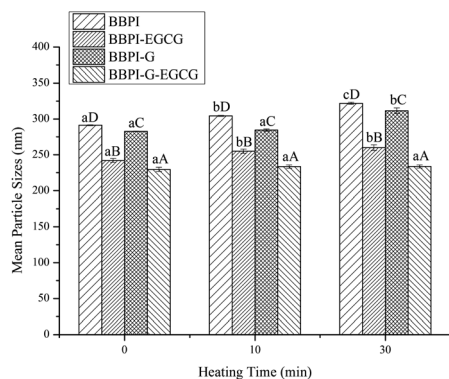


Fig. 6 Mean particle size of BBPI, BBPI-EGCG, BBPI-G, BBPI-G-EGCG emulsions with different heating time (10 and 30 min). a–c represent the significant difference in different heating time (min) with same emulsion. A–D means the significant difference in different emulsions with same heating time.

**3.3.3. Thermal stability of emulsions.** Many foods would undergo heat treatment during processing, such as pasteurization and ultra-high temperature short-time sterilization. Therefore, it is of great significance to investigate the effect of heating on emulsion stability. As revealed in Fig. 6, the mean particle size of the emulsion prepared with BBPI-G-EGCG covalent compound did not change significantly during the whole heat treatment period ( $p > 0.05$ ), explaining that the thermal stability of BBPI-G-EGCG emulsion was better than other emulsions (BBPI, BBPI-G, BBPI-EGCG emulsion). Liu *et al.*<sup>32</sup> found that after covalently combining lactoferrin with dextran, the thermal denaturation temperature of lactoferrin increased, which promoted the thermal stability of glycosylated lactoferrin emulsion. After binding with polyphenols, the adsorption capacity of proteins at oil–water interface was enhanced, resulting in thicker interfacial layer formed by protein–polyphenols complex and stronger spatial repulsive force, which benefited the thermal stability of the emulsion.<sup>5</sup>

**3.3.4. Freeze-thaw stability of emulsion.** Freezing storage of emulsion could inhibit the growth of microorganisms during

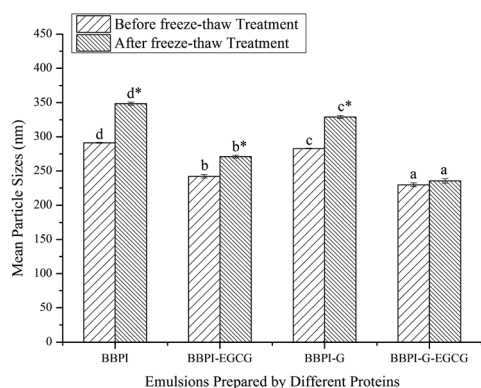


Fig. 7 Mean particle size of emulsions stabilized by BBPI, BBPI-EGCG, BBPI-G, BBPI-G-EGCG with freeze-thaw treatment or not. \* represent the significant difference in processing freeze-thaw treatment or not with same emulsion. a–d means the significant difference in different emulsions with same treatment.

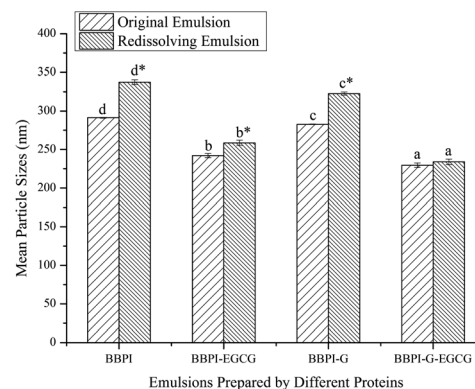


Fig. 8 Mean particle size of BBPI, BBPI-EGCG, BBPI-G, BBPI-G-EGCG emulsions before or after freeze-dried treatment. \* represent the significant difference in processing freeze-dried treatment or not with same emulsion. a–d means the significant difference in different emulsions with same treatment.

storage. Therefore, it was of practical significance to study the freeze–thaw stability of emulsions. As shown in Fig. 7, the mean particle size of the emulsion prepared by BBPI-G-EGCG covalent compound did not change significantly ( $p > 0.05$ ) after freeze–thaw treatment. This was because the compounding of sugar and protein generated thicker oil–water interface in emulsion, making it difficult to penetrate and rupture oil in water structure with the freeze–thaw treatment.<sup>52</sup> At the same time, a large number of hydroxyl groups were introduced into the protein molecules as the protein was combined with polyphenols, which promoted the increase of interfacial layer thickness of the emulsions, thus improving the freeze–thaw stability of the emulsions.<sup>46</sup>

**3.3.5. Resolubility of freeze-dried emulsion powder.** Storage life of the emulsion could be maximized by freeze-drying treatment. Hence, the resolubility of freeze-dried powder of emulsions was studied in this experiment. Different emulsion samples were freeze-dried into powder and then redissolved. The changes of mean particle size of the emulsions were shown in Fig. 8. The mean particle size of the emulsion prepared by BBPI-G-EGCG covalent compound did not change significantly ( $p > 0.05$ ). This was due to the addition of glucose, which enhanced the surface activity of BBPI, hence increasing the thickness of interface film and the spatial rejection. Therefore, the resolubility of freeze-dried powder of BBPI-G-EGCG emulsion was better.<sup>32</sup> After combining with polyphenols, the resolubility of freeze-dried powder of the emulsion could be improved by the increase of absolute zeta-potential of the emulsion, which further increased the electrostatic repulsion between droplets and promoted the anti-aggregation stability of the emulsion.<sup>53</sup>

## 4. Conclusions

In summary, this study provided the understanding of the behaviors for the potential applications of BBPI as emulsifiers in emulsions. FTIR spectroscopy showed that the structure of





protein was unfolded and disordered with the treatment of glycosylated and polyphenols covalent binding. The effects of the glycosylation and polyphenols modification on the stability of emulsions were investigated. The results showed that emulsions with considerable stability in storage, oxidation, thermal treatments, freeze-thaw and freeze-dried powders resolubility were fabricated. Small mean particle size of emulsion prepared by BBPI-G-EGCG was one reason for high emulsion stability. Besides, the AP and TEM measurements found that the BBPI-G-EGCG covalent complexes had a preferably thick, continuous, compact oil-water interface in emulsions, which was another factor to enhance the stability of emulsion systems. The results of this study provided new understanding with respect to using the modified black bean proteins as natural emulsifiers.

## Conflicts of interest

The authors declare no conflict of interest.

## Acknowledgements

This work was supported by the National Natural Science Foundation of China [No. 31901605], the Key Program of Natural Science Foundation of Heilongjiang Province [ZD2019C005] and Academic Backbone Project of Northeast Agricultural University [19XG27].

## References

- 1 Y. Zhang, Y. Yin and S. Lu, *Molecules*, 2018, **23**(9), 2127, DOI: 10.3390/molecules23092127.
- 2 L. Jiang, J. Wang, Y. Li, *et al.*, *Food Res. Int.*, 2014, **62**, 595–601, DOI: 10.1016/j.foodres.2014.04.022.
- 3 B. Xu and S. K. C. Chang, *J. Agric. Food Chem.*, 2008, **56**(18), 8365–8373, DOI: 10.1021/jf801196d.
- 4 H. Jin, C. Liu, S. Zhang, *et al.*, *Food Funct.*, 2020, **11**, 10205, DOI: 10.1039/D0FO01830A.
- 5 D. Li, Y. Zhao, X. Wang, *et al.*, *Food Hydrocolloids*, 2020, **98**, 105306, DOI: 10.1016/j.foodhyd.2019.105306.
- 6 J. Su, Q. Guo, Y. Chen, *et al.*, *Food Hydrocolloids*, 2020, **98**, 105293, DOI: 10.1016/j.foodhyd.2019.105293.
- 7 B. P. Loc, B. Wang, B. Zisu, *et al.*, *Food Chem.*, 2019, **293**, 463–471, DOI: 10.1016/j.foodchem.2019.04.123.
- 8 S.-D. Zhou, Y.-F. Lin and X. Xu, *Food Chem.*, 2020, **309**, 125718, DOI: 10.1016/j.foodchem.2019.125718.
- 9 J. Xu, D. Mukherjee and S. K. C. Chang, *Food Chem.*, 2018, **240**, 1005–1013, DOI: 10.1016/j.foodchem.2017.07.077.
- 10 F. Zha, S. Dong, J. Rao, *et al.*, *Food Chem.*, 2019, **285**, 130–138, DOI: 10.1016/j.foodchem.2019.01.151.
- 11 J.-C. Laura, M. Villamiel and L.-F. Rosina, *Food Hydrocolloids*, 2007, **21**(3), 433–443, DOI: 10.1016/j.foodhyd.2006.05.006.
- 12 L. Liu, J. Zheng, B. Sun, *et al.*, *Molecules*, 2020, **25**, 875, DOI: 10.3390/molecules25040875.
- 13 J. Xue, C. Tan, X. Zhang, *et al.*, *J. Agric. Food Chem.*, 2014, **62**(20), 4677–4684, DOI: 10.1021/jf405157x.
- 14 Z. Yu, L. Shuang, J. Zhang, *et al.*, *LWT-Food Sci. Technol.*, 2020, **125**, 109213, DOI: 10.1016/j.lwt.2020.109213.
- 15 M. Perusko, A. Al-Hanish, J. Mihailovic, *et al.*, *Food Chem.*, 2017, **232**, 744–752, DOI: 10.1016/j.foodchem.2017.04.074.
- 16 F. Liu, C. Sun, W. Yang, *et al.*, *RSC Adv.*, 2015, **5**(20), 15641–15651, DOI: 10.1039/c4ra10802g.
- 17 W. Chen, R. Lv, A. Muhammand, *et al.*, *Ultrason. Sonochem.*, 2019, **58**, 104678, DOI: 10.1016/j.ultsonch.2019.104678.
- 18 J. Xu, D. Han, Z. Chen, *et al.*, *Eur. Food Res. Technol.*, 2018, **244**(6), 1111–1120, DOI: 10.1007/s00217-018-3032-5.
- 19 Z. Wei and Q. Huang, *Food Hydrocolloids*, 2020, **98**, 105314, DOI: 10.1016/j.foodhyd.2019.105314.
- 20 K. Slinkard and V. L. Singleton, *Am. J. Enol. Vitic.*, 1977, **28**(1), 49–55, DOI: 10.1002/star.19780301107.
- 21 Y. Wang, Z. Wang, C. L. Handa, *et al.*, *Food Chem.*, 2017, **218**, 165–172, DOI: 10.1016/j.foodchem.2016.09.069.
- 22 M. Carbonaro, P. Maselli and A. Nucara, *Amino Acids*, 2012, **43**, 911–921, DOI: 10.1007/s00726-011-1151-4.
- 23 H. Jin, Q. Zhao, H. Feng, *et al.*, *Polymers*, 2019, **11**(5), 848, DOI: 10.3390/polym11050848.
- 24 H. Jin, X. Wang, Z. Chen, *et al.*, *Food Res. Int.*, 2018, **106**, 800–808, DOI: 10.1016/j.foodres.2018.01.056.
- 25 Y. Li, H. Jin, X. Sun, *et al.*, *Nanomaterials*, 2018, **9**(1), 25, DOI: 10.3390/nano9010025.
- 26 M. Chen, J. Lu, F. Liu, *et al.*, *Food Hydrocolloids*, 2019, **88**, 247–255, DOI: 10.1016/j.foodhyd.2018.09.003.
- 27 O. H. Lowry, N. J. Rosebrough, A. L. Farr, *et al.*, *J. Biol. Chem.*, 1951, **193**(1), 265–275, DOI: 10.1515/bchm2.1951.286.1-6.270.
- 28 H. Feng, H. Jin, Y. Gao, *et al.*, *Polymers*, 2019, **11**(10), 1688, DOI: 10.3390/polym11101688.
- 29 Y. Yang, S. Cui, J. Gong, *et al.*, *Food Res. Int.*, 2015, **69**, 357–363, DOI: 10.1016/j.foodres.2015.01.006.
- 30 L. Y. Mei, D. J. McClements, J. N. Wu, *et al.*, *Food Chem.*, 1998, **61**, 307–312, DOI: 10.1016/S0308-8146(97)00058-7.
- 31 H. Feng, H. Jin, Y. Gao, *et al.*, *Food Chem.*, 2020, **330**, 127215, DOI: 10.1016/j.foodchem.2020.127215.
- 32 F. Liu, C. Ma, D. J. McClements, *et al.*, *Food Hydrocolloids*, 2016, **61**, 578–588, DOI: 10.1016/j.foodhyd.2016.05.031.
- 33 X. Sui, H. Sun, B. Qi, *et al.*, *Food Chem.*, 2018, **245**, 871–878, DOI: 10.1016/j.foodchem.2017.11.090.
- 34 M. Ali, T. Homann, M. Khalil, *et al.*, *J. Agric. Food Chem.*, 2013, **61**(28), 6911–6920, DOI: 10.1021/jf402221m.
- 35 V. Bongartz, L. Brandt, M. L. Gehrman, *et al.*, *Molecules*, 2016, **21**(1), 91, DOI: 10.3390/molecules21010091.
- 36 Z. Wei, W. Yang, R. Fan, *et al.*, *Food Hydrocolloids*, 2015, **45**, 337–350, DOI: 10.1016/j.foodhyd.2014.12.008.
- 37 J. Wagner and J. Gueguen, *J. Agric. Food Chem.*, 1999, **47**(6), 2181–2187, DOI: 10.1021/jf980977b.
- 38 Y. Li, H. Liu, Q. Liu, *et al.*, *Food Hydrocolloids*, 2019, **87**, 149–157, DOI: 10.1016/j.foodhyd.2018.07.052.
- 39 C. Liu, Z. Wang, H. Jin, *et al.*, *Int. J. Biol. Macromol.*, 2019, **142**, 658–667, DOI: 10.1016/j.ijbiomac.2019.10.007.
- 40 C. Sarah and D.-P. Gabriel, *Food Chem.*, 2020, **338**, 128083, DOI: 10.1016/j.foodchem.2020.128083.
- 41 J. Jiang and Y. L. Xiong, *Meat Sci.*, 2015, **109**, 56–65, DOI: 10.1016/j.meatsci.2015.05.011.



- 42 J. Chen, Y. Feng, B. Kong, *et al.*, *Colloids Surf., A*, 2020, **604**, 125332, DOI: 10.1016/j.colsurfa.2020.125332.
- 43 L. Atares, L. J. Marshall, M. Akhtar, *et al.*, *Food Chem.*, 2012, **134**(3), 1418–1424, DOI: 10.1016/j.foodchem.2012.02.221.
- 44 J. Chen, Y. Feng, B. Kong, *et al.*, *Food Hydrocolloids*, 2015, **51**, 95–100, DOI: 10.1016/j.foodhyd.2015.04.034.
- 45 F. Liu, D. Wang, H. Xu, *et al.*, *Food Chem.*, 2016, **196**, 338–346, DOI: 10.1016/j.foodchem.2015.09.047.
- 46 Y. H. Wang, Z. L. Wan, X. Q. Yang, *et al.*, *Food Hydrocolloids*, 2016, **54**, 40–48, DOI: 10.1016/j.foodhyd.2015.09.020.
- 47 L. Wang and Y. Xiong, *J. Agric. Food Chem.*, 2005, **53**(23), 9186–9192, DOI: 10.1021/jf051213g.
- 48 C. Liu, H. Jin, Y. Yu, *et al.*, *Nanomaterials*, 2020, **10**(6), 1094, DOI: 10.3390/nano10061094.
- 49 S. Dong, A. Panya, M. Zeng, *et al.*, *Food Res. Int.*, 2013, **51**(2), 992, DOI: 10.1016/j.foodres.2013.03.033.
- 50 M. Verni, V. Verardo and C. G. Rizzello, *Foods*, 2019, **8**(9), 362, DOI: 10.3390/foods8090362.
- 51 D. K. Sarker, P. J. Wilde and D. C. Clark, *J. Agric. Food Chem.*, 1995, **43**, 295–300, DOI: 10.1021/jf00050a006.
- 52 Z. Zhang, X. Wang, J. Yu, *et al.*, *LWT–Food Sci. Technol.*, 2017, **78**, 241–249, DOI: 10.1016/j.lwt.2016.12.051.
- 53 Y. Chen, C. Wang, H. Liu, *et al.*, *Colloids Surf., A*, 2018, **558**, 330–337, DOI: 10.1016/j.colsurfa.2018.08.067.

